https://doi.org/10.24191/jeesr.v20i1.007

EEG-based IQ Pattern Analysis: Considerations on Filter Design and Power Ratio Equations

Najwa Ahmad Suhaimi, Ahmad Ihsan Mohd Yassin, Megat Syahirul Amin Megat Ali* and Aisyah Hartini Jahidin

Abstract—**Intelligence is defined as the mental ability to learn, reason and solve problems. Recently, studies have characterized the different levels of intelligence quotient from the resting brainwaves. Various filter designs and power ratio equations have been proposed, all with unique strengths and limitations. Hence, further investigation is required to standardize the pre-processing algorithm using the established electroencephalogram database. The previously established Hamming and equiripple filter designs are evaluated in this study. The later are more superior for filtering the electroencephalogram into the respective brainwaves. Despite the limitations, the low-order Hamming filters are still recommended as the memory required is only 6% of the high-order equiripple filters. These greatly enhance the computational efficiency. The cross-correlation function tests further revealed the impact of filter designs on the resultant brainwaves. Hence, a new set of power ratio equations have been successfully formulated for dataset validation.**

Index Terms—**EEG, equiripple filter, Hamming filter, IQ, power ratio.**

I. Introduction

INTELLIGENCE can be broadly defined as the mental ability for reasoning, problem solving, and learning. Generally, the trait integrates cognitive functions such as memory, attention, perception, planning and language [1]. Intelligence can be measured using standardized tests and the scores are used to predict board social outcomes such as educational achievement, adaptive competencies, job performance, and personality types [2]. Psychometric test batteries such as Raven's Progressive Matrices (RPM) [3] and Weschler's Intelligence Scale [4] can be used to assess the ability, which is commonly measured as of intelligence quotient (IQ). Despite its widespread adoption, the conventional testing methods are still exposed to bias issues [5]. The procedure is time-consuming and must be administered by qualified psychologists [3]. To solve these shortcomings, studies have proposed an alternative method to classify IQ level from the resting electroencephalogram (EEG) [6].

These have been realized using power ratio features and computational models developed using artificial neural network and support vector machines [7, 8]. The proposed power ratio features in theta, alpha, and beta bands have shown conformity with the Neural Efficiency Hypothesis, thereby allowing the model to learn and generalize the features for different IQ levels [9]. Bright individuals demonstrate lower brain activation than the less intelligent ones, which are then reflected in higher alpha power. The increased synchronization effectively reduces the brainwave oscillations in theta and beta regions [10]. Hence, bright people will generally exhibit relatively higher alpha, but lower theta and beta ratio compared to the less intelligent individuals [11]. Further investigation also showed a variation in the power ratio equations and these are very much related to the filters being used.

Initially, a low-order filter designed with Hamming window was proposed. The use of Hamming filter resulted in power ratio equations that do not consider the interaction between all frequency bands of interest [9]. Thus, an alternative filter design was later proposed through optimal design method. These led to the adoption of high-order equiripple filters with superior filtering capabilities. The power ratio equations were then revised to consider the interaction between theta, alpha and beta bands. However, the order of the filter is extremely high. These require higher memory capacity and increases computational load for EEG pre-processing [12]. Therefore, a re-evaluation on the filter designs and power ratio equations are required for developing optimal EEG pre-processing algorithm.

II. Methods

A. Data Acquisition

The EEG are obtained from previously established database, approved by the Research Ethics Committee of Universiti Teknologi MARA [7]. Subjects were comprised of 21 males and and 29 females. They have been screened to comply with the inclusion criteria and given written consent. Participants are right-handed and were not under any prescribed medications. They were from different educational disciplines with age range of between 20 to 40 years old. The resting EEG were acquired

This manuscript is submitted on 8th November 2021 and accepted on 3th Feb 2022. This work was supported in part by Universiti Teknologi MARA through the LESTARI research grant (600-IRMI 5/3/LESTARI (032/2019)).

Najwa Ahmad Suhaimi is with Kumpulan Abex Sdn. Bhd., 40400 Shah Alam, Selangor, Malaysia. She is also a postgraduate student at the College of Engineering, Universiti Teknologi MARA, 40450 Shah Alam, Malaysia.

Ahmad Ihsan Mohd Yassin and Megat Syahirul Amin Megat Ali are with the Microwave Research Institute, Universiti Teknologi MARA, 40450 Shah Alam, Malaysia (megatsyahirul@uitm.edu.my)

Aisyah Hartini Jahidin is with the Centre for Foundation Studies in Science, University of Malaya, 50603 Kuala Lumpur, Malaysia.

*Corresponding author
Email address: megatsyahirul@uitm.edu.my

from the left prefrontal cortex while the subjects are relaxed in seated position with both eyes closed. Three minutes EEG were recorded using g.MOBIlab+ at sampling frequency of 256 Hz. The EEG from database were clustered into high, medium and low IQ level groups. The segregations were made based on the scores obtained from RPM-based IQ test. Based on information obtained, the high IQ level group consists of 6 samples. Meanwhile, 39 samples belong to the medium IQ level group, and low IQ level consists of 5 samples.

B. *Hamming and Equiripple Filters*

Two finite impulse respone filter designs are adopted in this study. The low-order filter developed using Hamming window and equiripple filter that was designed with Parks-McClellan algorithm. Fig. 1, Fig. 2, and Fig. 3 each shows the reproduced magnitude response plots of the Hamming filter for theta, alpha and beta bands [12]. The low filter order of 74 resulted in wide transition band. Stop-band attenuation for Hamming window is at –54 dB. Therefore, spectral leakages are expected near the band edges of the filtered brainwaves.

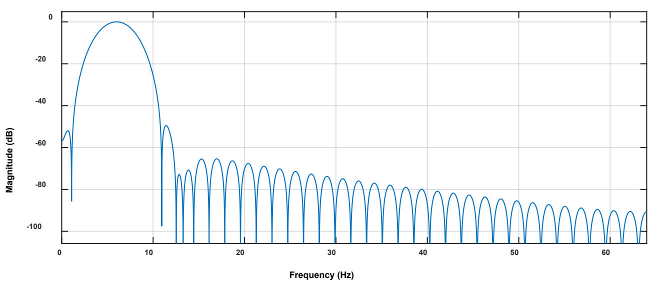

Fig. 1. Magnitude response of Hamming filter (N=74) for theta wave.

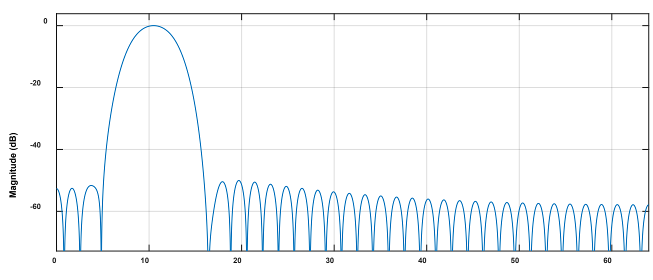

Fig. 2. Magnitude response of Hamming filter (N=74) for alpha wave.

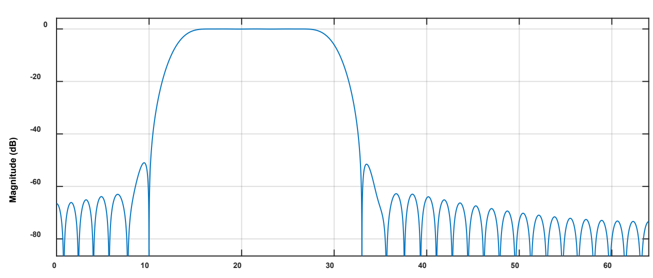

Fig. 3. Magnitude response of Hamming filter (N=74) for beta wave.

Meanwhile, the equiripple filter was designed with a more stringent set of constraints. A steep transition band of 0.2 Hz with stop-band attenuation of –60 dB was proposed to reduce spectral leakage of the filtered brainwaves. The desgins were realized through Parks-McClellan algorithm, resulting in a very high filter order of 1264. Comparatively, each equiripple filter requires 17 times more memory than the preceding Hamming filters. Fig. 4, Fig. 5, and Fig. 6 each shows the reproduced magnitude response plots of the equiripple filter for theta, alpha

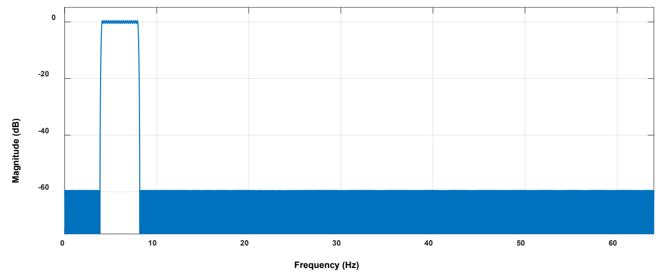

Fig. 4. Magnitude response of equiripple filter (N=1264) for theta wave.

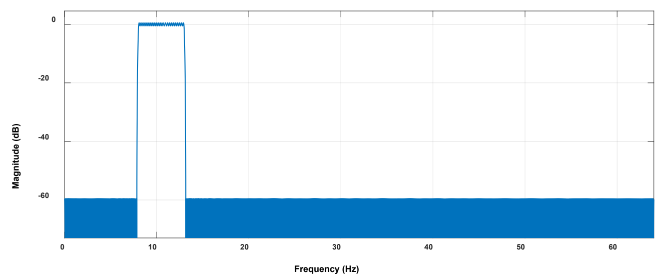

Fig. 5. Magnitude response of equiripple filter (N=1264) for alpha wave.

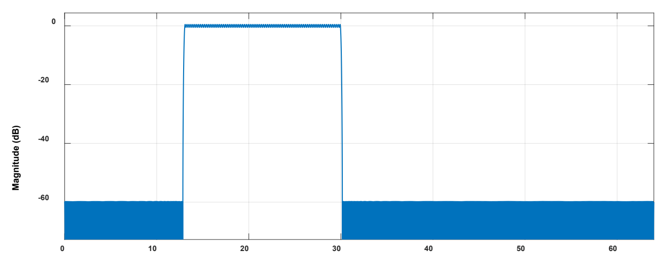

Fig. 6. Magnitude response of equiripple filter (N=1264) for beta wave.

and beta bands [12].

Two EEG pre-processing algorithms are then developed; one with Hamming filters and the other with equiripple filters. The function files loaded when segregating the EEG into the respective brainwaves.

C. *EEG Pre-Processing and Power Ratio Equations*

Baseline correction is initially performed on the loaded EEG. Any epoch with amplitudes exceeding ±100 µV is considered as electrooculogram (EOG) artifacts and removed through rejection method. Subsequently, the duration is standardized to 2 minutes and 30 seconds. The EEG is then segregated into theta, alpha and beta waves using the designed filters. Estimation of the non-parametric power spectrum density (PSD) is performed through Welch method. Consequently, energy spectral density (ESD) for the respective bands are calculated as the area under PSD curve per unit frequency.

The obtained ESD are then normalized through the power ratio equations. In earlier study employing low-order Hamming filters, the parameters are computed using (1), (2) and (3). θ, α, and β each represented the ESD in theta, alpha and beta bands. Hence, the equations demonstrate that the denominators do not consider the interaction between all EEG bands of interest.

$$\text{Theta Ratio} = \frac{\theta}{\theta + \alpha} \tag{1}$$

$$\text{Alpha Ratio} = \frac{\alpha}{\alpha + \beta} \tag{2}$$

$$\text{Beta Ratio} = \frac{\beta}{\alpha + \beta} \tag{3}$$

Meanwhile, the succeeding study with high-order equiripple filters proposed a revision to the power ratio equations. These are shown by (4), (5) and (6). The denominators used in now considers the behaviour of ESD in theta, alpha and beta bands. The proposed revision to the equation still complies with the Neural Efficiency Hypothesis. The pattern of power ratio for the respective bands have been evaluated through box plot analysis.

$$\text{Theta Ratio} = \frac{\theta}{\theta + \alpha + \beta} \tag{4}$$

$$\text{Alpha Ratio} = \frac{\alpha}{\theta + \alpha + \beta} \tag{5}$$

$$\text{Beta Ratio} = \frac{\beta}{\theta + \alpha + \beta} \tag{6}$$

To further assess the effectiveness of the revised power ratio equation, the a cross-correlation function tests are proposed for this study. Correlation analysis is used to determine the dependency between two variables. The correlation coefficient, r_{xy}, between variables x and y is shown by (7).

$$r_{xy} = \frac{\sum \left(x_i - \bar{x} \right) \left(y_i - \bar{y} \right)}{\sqrt{\sum \left(x_i - \bar{x} \right)^2 \left(y_i - \bar{y} \right)^2}} \tag{7}$$

The cross-correlation is used to measure the similarity of two brainwaves as a function of the displacement of one brainwave, relative to the other. For both brainwaves to be correlated, the coefficients must exceed the 95% confidence interval limit. As shown in (8), the intervals, Δ, are affected by the number of sample points, N.

$$\Delta = \pm \frac{1.96}{\sqrt{N}} \tag{8}$$

III. Results and Discussion

A. Filtered Brainwaves

The algorithm has been sufficiently be written to perform baseline correction, EOG rejection, and segregation of the EEG into the desired brainwaves. Fig. 8 and Fig. 9 shows an eight-second segment of theta waves extracted with Hamming and equiripple filters. Both samples indicate similarity in terms oscillation pattern. The amplitude range is approximately ±15 μV with consistent distance between each cycle of oscillation.

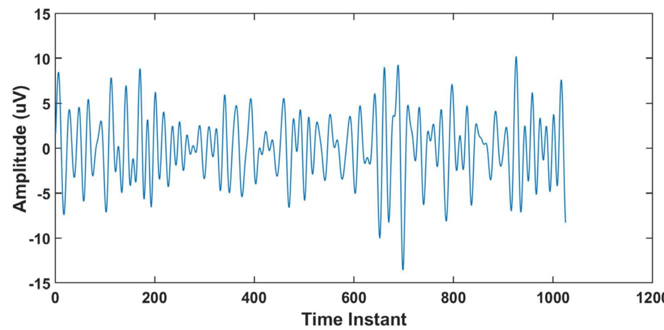

Fig. 7. Theta waves filtered using Hamming filter (N=74).

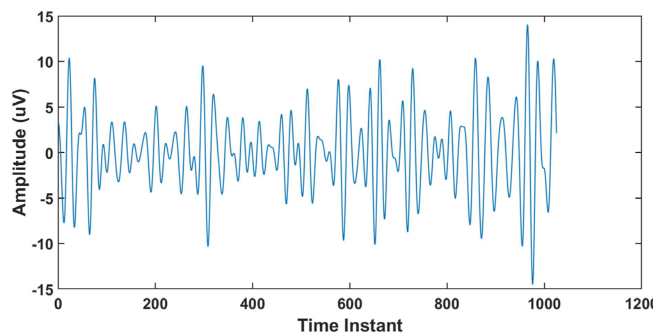

Fig. 8. Theta waves filtered using equiripple filter (N=1264).

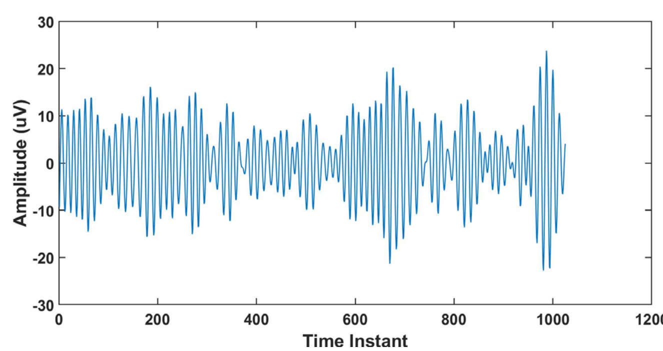

Fig. 9. Alpha waves filtered using Hamming filter (N=74).

Meanwhile, Fig. 9 and Fig. 10 each shows an eight-second segment of alpha wave that was extracted using Hamming and equiripple filters. Both samples show similar oscillation pattern. The amplitude range is ±25 μV with each cycle of oscillation

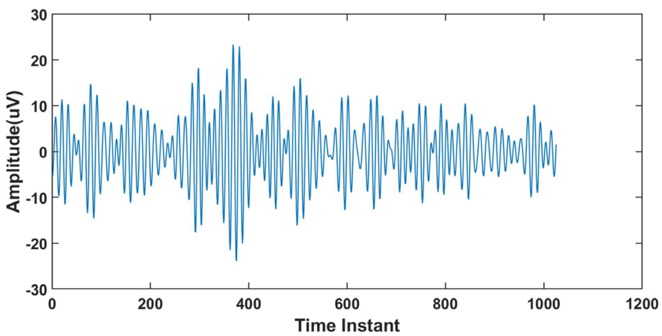

Fig. 10. Alpha waves filtered using equiripple filter (N=1264).

having consistent distance. The distance however, are much closer compared to the theta waves, confirming the increased frequency range of the alpha band.

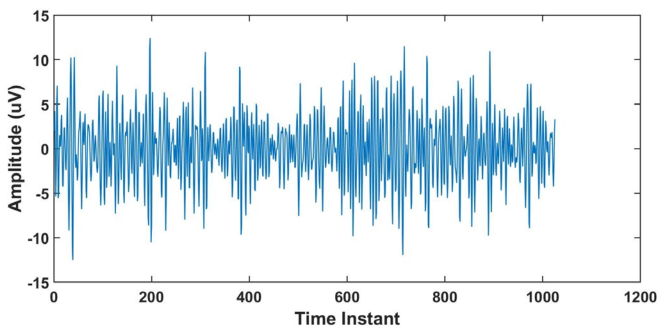

Fig. 11. Beta waves filtered using Hamming filter (N=74).

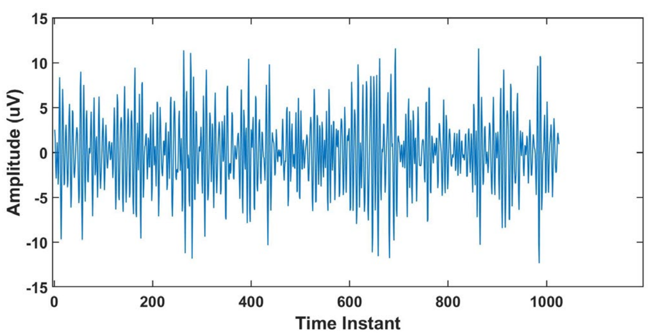

Fig. 12. Beta waves filtered using equiripple filter (N=1264).

Similarly, Fig. 11 and Fig. 12 each shows an eight-second segment of beta wave that was extracted using Hamming and equiripple filters. Both samples exhibit similar pattern of oscillation. The amplitude range is ±15 μV with consistent distance between the cycles of oscillation. The distance that each much closer than the oscillation of alpha waves confirms the higher frequency range of the beta band.

The visual inspection time-series representation of theta, alpha and beta waves did not reveal the impact of both filter designs. Therefore, the respective brainwaves are converted to PSD through Welch method. The PSD for theta, alpha and beta waves extracted using Hamming filters are shown in Fig. 13.

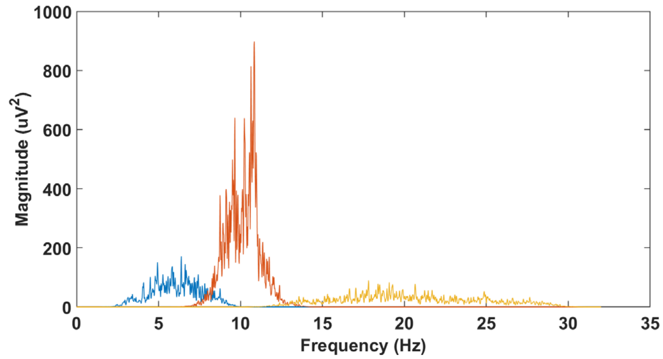

Fig. 13. PSD for theta (blue), alpha (orange) and beta (yellow) waves extracted using Hamming filters.

The plot shows that information is more truncated near the band edges. The overlapping region between each band is also evident, which increases spectral leakage spreading into the adjacent frequency bands. Generally, Hamming filters have successfully extracted the theta, alpha, and beta waves, albeit less efficient.

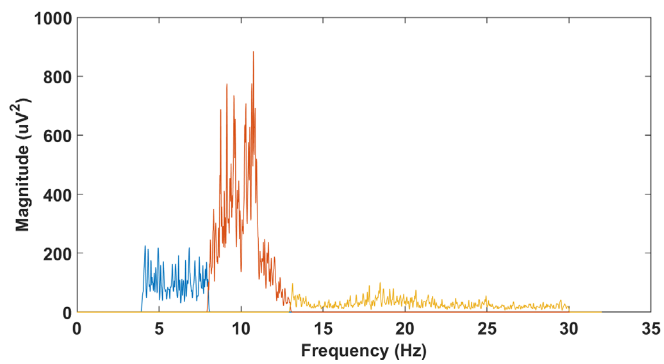

Fig. 14. PSD for theta (blue), alpha (orange) and beta (yellow) waves extracted using equiripple filters.

Meanwhile, PSD for theta, alpha and beta waves extracted using Hamming filters are shown in Fig. 14. Comparatively, the plot shows minimal truncation of information near the band edges. Spectral leakage is also significantly reduced with minimum overlapping region between the adjacent bands. This shows that equiripple filters have efficiently extracted the theta, alpha, and beta waves, albeit the high memory requirement.

B. *Conformity with Neural Efficiency Hypothesis*

Box plots are used to assess the conformance of the power ratio features with the Neural Efficiency Hypothesis of human intelligence. The analysis is based on a dataset with size of 50 samples. The evaluation focuses on the median of theta, alpha and beta ratio among the three IQ level groups. Generally, the high IQ level group should have the highest median for alpha ratio. This is followed by medium and then, the low IQ level group. The pattern however, is negatively correlated with the other two frequency bands. The high IQ level group should attain the lowest median for theta and beta ratio. These are then

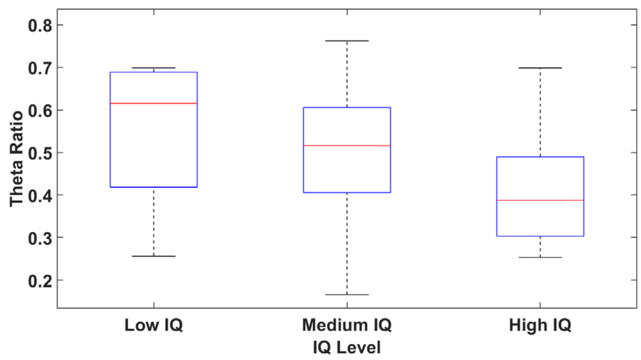

Fig. 15. Box plot for theta ratio features extracted using Hamming filters (N=50).

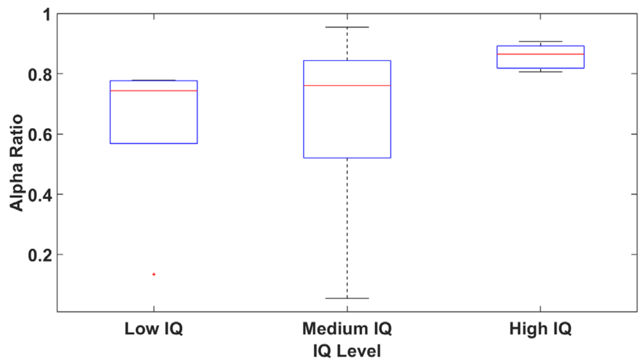

Fig. 16. Box plot for alpha ratio features extracted using Hamming filters (N=50).

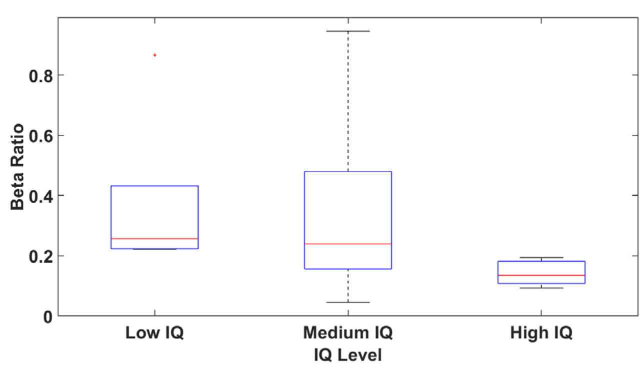

Fig. 17. Box plot for beta ratio features extracted using Hamming filters (N=50).

followed by medium and then, the low IQ level group.

Fig. 15, Fig. 16, and Fig. 17 each shows the box plot for theta alpha and beta ratio extracted using Hamming filters. The computation of power ratio features are based on the equations shown by (1), (2) and (3). Generally, the features demonstrate conformity with the Neural Efficiency Hypothesis of human intelligence and has good discriminative ability. One outlier has been observed for alpha and beta ratio in the low IQ level group.

Meanwhile, Fig. 18, Fig. 19, and Fig. 20 each shows the box plot for theta, alpha and beta ratio extracted using equiripple filters. Do note that the power ratio is calculated based on the revised equations given by (4), (5) and (6). Similarly, the features demonstrate conformity with the Neural Efficiency Hypothesis of human intelligence. However, eight outliers have

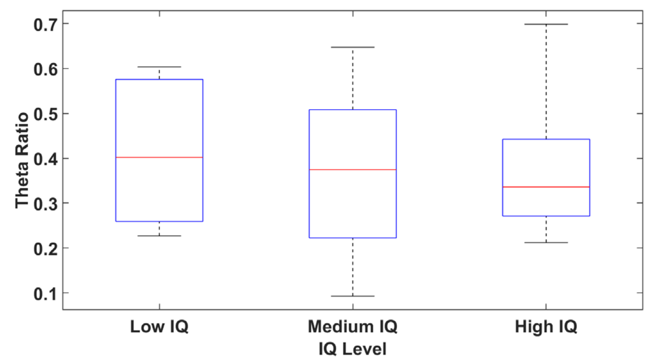

Fig. 18. Box plot for theta ratio features extracted using equiripple filters (N=50).

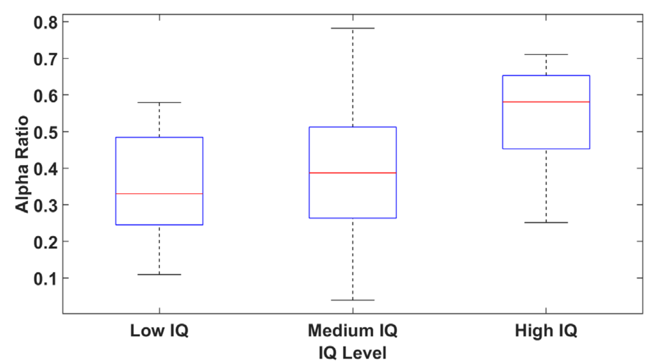

Fig. 19. Box plot for theta ratio features extracted using equiripple filters (N=50).

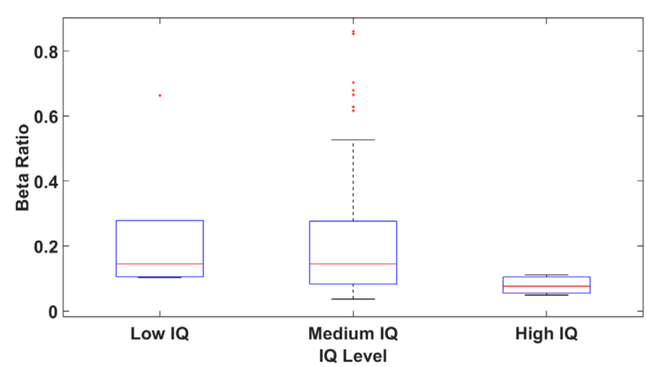

Fig. 18. Box plot for theta ratio features extracted using equiripple filters (N=50).

been identified for beta ratio features; seven in the medium IQ level and one in the low IQ level group.

Detailed investigation has also revealed that the median of beta ratio for medium IQ level deviates from the low IQ level group by a mere 0.03%. Contrariwise, the smallest deviation between the median values attained using the earlier version of power ratio equation is at 7%, which also occurred for beta ratio feature between medium IQ level and low IQ level groups.

Therefore, the normalized feature may not fully represent the behavior of beta band for differentiating between medium IQ level and low IQ level groups. These permit an investigation on the validity of the revised version of the power ratio equations.

C. Cross-Correlation Function Test

The effects of using Hamming and equiripple filters on the pre-processed EEG are futher analyzed using cross-correlation function test. For each filter design, the analysis is performed between the following brainwaves; theta-alpha, alpha-beta, and theta-beta pairs. As previously mentioned, the brainwaves of different frequency bands are correlated if the coefficients exceed the 95% confidence interval. The limits denoted by the horizontal blue line in the correlogram.

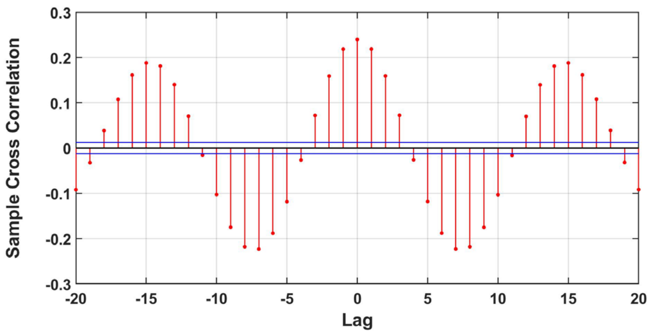

Fig. 19. Correlogram for theta-alpha pairs extracted with Hamming filters.

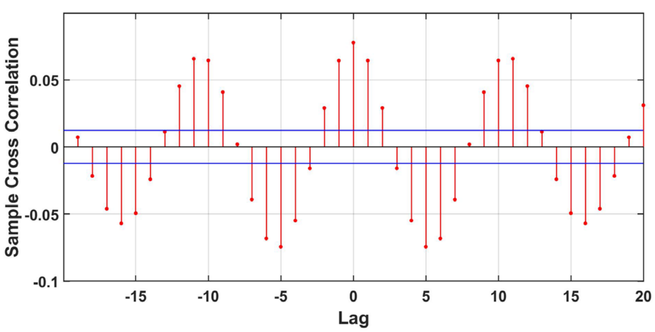

Fig. 20. Correlogram for alpha-beta pairs extracted with Hamming filters.

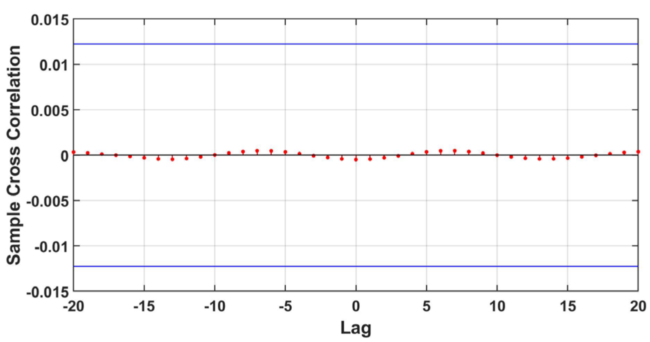

Fig. 21. Correlogram for theta-beta pairs extracted with Hamming filters.

The correlogram of theta-alpha, alpha-beta, and theta-beta pairs extracted using Hamming filters are each shown in Fig. 19, Fig. 20, and Fig. 21. Generally, the coefficients yielded an oscillatory pattern with increasing lags which suggests periodic relationship between the brainwave pairing. By inspecting the coefficients and the confidence interval limits, only theta-alpha, and alpha-beta pairs are correlated. The theta-beta pair is not correlated as all coefficients fall within the confidence interval.

The low-order Hamming filters are less effective for filtering the brainwaves. Therefore, the observation is valid as spectral leakages between theta and alpha band resulted in increased correlation. Similar deduction can be drawn for alpha and beta waves. However, the peak coefficient values are much lower as beta band contains more frequency component than theta band. Meanwhile, alpha band acted as a buffer zone between theta and beta frequency ranges. This effectively renders both bands to be uncorrelated.

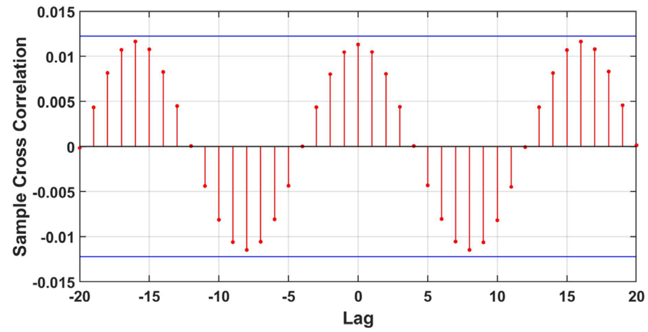

Fig. 22. Correlogram for theta-alpha pairs extracted with equiripple filters.

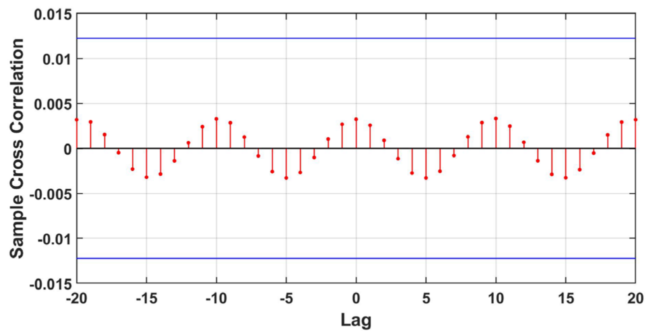

Fig. 23. Correlogram for alpha-beta pairs extracted with equiripple filters.

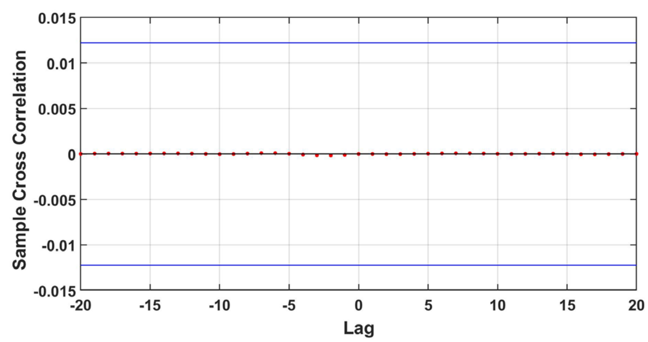

Fig. 24. Correlogram for theta-beta pairs extracted with equiripple filters.

Comparatively, the correlogram for theta-alpha, alpha-beta, and theta-beta pairs extracted using equiripple filters are each shown in Fig. 22, Fig. 23, and Fig. 24. The coefficients for all brainwave pairing indicated oscillatory pattern. These are similar with the results attained with Hamming filters, with a major difference in peak coefficient values. By considering the confidence interval, none of the brainwaves are correlated with one another.

The high-order equiripple filters have effectively filtered the brainwaves, minimizing the spectral leakage and reduces the overlapping region between the adjacent bands. These effectively reduces the peak coefficient values for theta-alpha and alpha-beta pairs to within the confidence interval limit. Similarly with the preceding results, the peak coefficient values for alpha-beta correlation is lower than the theta-alpha pair. Also, the theta-beta pair remains uncorrelated with the lower peak coefficient values.

D. Considerations on Power Ratio Equations

The preceding results have demonstrated the effectiveness of equiripple filters for segregating the EEG into the respective brainwaves. However, the use of these high-order filter designs significantly increase the computational load. To mitigate these issues, the study still recommends the use of low-order Hamming filters. These will reduce the memory requirement and increases computational efficiency in the pre-processing algorithm.

However, the previously established power ratio equations will have to be re-evaluated. The normalization method has to consider the relationship between alpha band with the adjacent theta and beta bands. The power ratio equations shown by (9), (10), and (11), are thereby proposed for dataset validation. Note that these are integrated into the EEG pre-processing algorithm together with the Hamming filters.

$$\text{Theta Ratio } = \frac{\theta}{\theta + \alpha} \tag{9}$$

$$\text{Alpha Ratio } = \frac{\alpha}{\theta + \alpha + \beta} \tag{10}$$

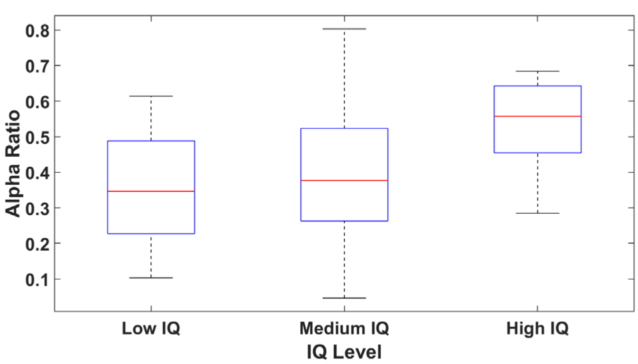

Fig. 25. Box plot for the new alpha ratio features extracted using Hamming filters (N=50).

$$\text{Beta Ratio } = \frac{\beta}{\alpha + \beta} \tag{11}$$

By adopting the new normalization equation, the alpha ratio distribution for different IQ levels is shown in Fig. 25. The pattern of median still maintains compliance with the Neural Efficiency Hypothesis while maintaining good discriminative ability. Furthermore, no outlier has been observed.

IV. CONCLUSION

The study has set out to investigate the previously proposed filter designs and power ratio equations for EEG-based IQ pattern analysis. Initially, the investigation analyzed the impact of using low-order Hamming filter and high-order equiripple filter designs. The later has demonstrated superior capability for segregating the EEG into theta, alpha and beta waves. These are attributed by the frequency response that preserves information near the band edges whilst minimizing the spectral leakages. However, the high filter order imposes increased computational load. Furthermore, the resultant beta ratio features have poor discriminative ability between the medium IQ level and low IQ level groups.

To overcome such limitations, the study recommends the use of low-order Hamming filters for reduced memory requirement and increased computational efficiency in the pre-processing algorithm. Generally, the design only impose 6% memory requirement compared to that of the equiripple filters. Also, the power ratio equations show good discriminative ability between all IQ level groups. The cross-correlation function tests for different brainwave pairing revealed that the established alpha ratio equation had to be re-evaluated. The normalization now considers the interaction of the alpha band with the two adjacent theta and beta bands.

Together with the Hamming filters, a new set of power ratio equations are proposed to validate dataset compliance with Neural Efficiency Hypothesis of human intelligence. Also, the cross-correlation function tests revealed a periodic relationship between theta, alpha, and beta waves. These indicate the inter-dependency between the time-series information at different lags and can thereby, be modelled using advanced deep learning methods.

ACKNOWLEDGEMENT

Authors would like to thank Research Management Centre, Universiti Teknologi MARA for funding this study through the LESTARI grant (600-IRMI 5/3/LESTARI (032/2019)).

REFERENCES

[1] R. Colom, S. Karama, R. E. Jung, and R. J. Haier, "Human intelligence and brain networks," *Dialogues Clin. Neurosci.*, vol. 12, no. 4, pp. 489–501, 2010.

[2] A. Furnham, J. Moutafi, and T. Chamorro-Premuzic, "Personality and intelligence: Gender, the Big Five, self-estimated and psychometric intelligence," *Int. J. Sel. Assess.*, vol. 13, no. 1, pp. 11–24, 2005.

[3] J. W. H. McLeod and A. W. McCrimmon, "Test review: Raven's 2 Progressive Matrices, Clinical Edition (Raven's 2)," *J. Psychoeduc. Assess.*, vol. 39, no. 3, pp. 388–392, 2020.

[4] M. Lang, M. Matta, L. Parolin, C. Morrone, and L. Pezzuti, "Cognitive profile of intellectually gifted adults: Analyzing the Wechsler Adult Intelligence Scale," *Assess.*, vol. 26, no. 5, pp. 929–943, 2019.

[5] L. Gottfredson and D. H. Saklofske, "Intelligence: Foundation and issues in assessment," *Can. Psychol.*, vol. 50, no. 3, pp. 183–195, 2009.

[6] A. H. Jahidin, M. N. Taib, M. S. A. Megat Ali, N. Md Tahir, S. Lias, M. H. Haron, R. Mohd Isa, W. R. W. Omar, and N. Fuad, "Evaluation of brainwave sub-band spectral centroid in human intelligence," in *2013 IEEE 9th Int. Colloq. Signal Process. Its Appl.*, 2013, pp. 295–298.

[7] A. H. Jahidin, M. S. A. Megat Ali, M. N. Taib, N. Md Tahir, I. M. Yassin, and S. Lias, "Classification of intelligence quotient via brainwave sub-

band power ratio features and artificial neural network," *Comput. Methods Programs Biomed.*, vol. 114, no. 1, pp. 50–59, 2014.

[8] N. J. Ros Azamin, M. N. Taib, A. H. Jahidin, D. S. Awang, and M. S. A. Megat Ali, "IQ level prediction and cross-relational analysis with perceptual ability using EEG-based SVM classification model," *IAES Int. J. Artif. Intell.*, vol. 8, no. 4, pp. 436–443, 2019.

[9] A. H. Jahidin, M. N. Taib, N. Md Tahir, M. S. A. Megat Ali, S. Lias, N. Fuad, and W. R. W. Omar, "Brainwave sub-band power ratio characteristics in intelligence assessment," in *2012 IEEE Control Syst. Grad. Res. Colloq.*, 2012, pp. 318–321.

[10] A. C. Neubauer and A. Fink, "Intelligence and neural efficiency," *Neurosci. Biobehav. Rev.*, vol. 33, no. 7, pp. 1004 – 1023, 2009.

[11] D. Nussbaumer, R. H. Grabner, and E. Stern, "Neural efficiency in working memory tasks: The impact of task demand," *Intell.*, vol. 50, pp. 196–208, 2015.

[12] N. H. Ros Azamin, A. H. Jahidin, M. S. A. Megat Ali, and M. N. Taib, "Enhancement of filter design and EEG power ratio features in IQ pattern analysis," *Int. J. Electr. Electron. Syst. Res.*, vol. 11, 2017.